Computing Two-fluid Models of Compressible Water-vapour Flows with Mass Transfer

Jean-Marc Hérard, Olivier Hurisse

Computing Two-Fluid Models of Compressible Water-Vapour Flows with Mass Transfer

Jean-Marc Hérard*
EDF, R&D, 6 quai Watier, 78400, Chatou, France.
Olivier Hurisse †
EDF, R&D, 6 quai Watier, 78400, Chatou, France.

We focus in this paper on the computation of two-fluid models of compressible water-vapour flows with mass transfer. Once the model and its main properties have been recalled, we detail the whole algorithm with special emphasis on the schemes that give approximate solutions of the source terms. Some recent results are eventually presented.

I. Introduction

This paper is devoted to the simulation of water-vapour flows with mass transfer, using the two-fluid approach proposed in[4,5,8,11,12,17,22,23,27] . The two-fluid model contains stiff source terms associated with pressure-velocity-temperature-Gibbs potential relaxation terms, and the convective part of the model is highly non linear and has no conservative form. Thus the computation of the whole model is rather difficult, and it requires the development of specific algorithms. Actually, a rather slow rate of convergence of schemes with respect to the mesh size is expected for convection-dominated flow computations (more precisely $h^{1/2}$ -respectively $h^{2/3}$- for so-called first-order -respectively second-order- schemes) , due to the occurence of several contact discontinuities, and the reader is refered to references[1,2,7,9,13,25,26,28,30,31] for instance, which examine in detail the behaviour of several Riemann solvers and relaxation techniques in order to cope with the convective part of the two-fluid model. Moreover, small time scales in relaxation source terms render the computation even more tricky, and some attempts to deal with pressure-velocity-temperature relaxation effects have been recently reported in[20,21] . One difficulty is connected with the computation of pressure relaxation effects, since it requires a tight coupling of source terms in energy and statistical void fraction equations. The accurate computation of gas-liquid flows with no mass transfer is not easy, but water-vapour flow simulations that account for mass transfer are clearly even more difficult, and emphasis is given here on this topic.

The paper will be organized as follows. We will first recall the set of PDEs that governs the two-fluid model. Next we will present the fractional step algorithm that is used in order to compute approximations of solutions of the whole system. The most difficult task dwells in the building of suitable algorithms in the pressure relaxation step. The section of numerical results will first recall some recent measurements of convergence rates, and then we will focus on the effect of mass transfer in two different situations.

II. Governing equations of the two-fluid model

Throughout the paper, indexes l, v refer to the liquid and vapour phases ; the statistical void fractions of vapour and liquid are noted classically α_v and α_l, which should agree with:

$$\alpha_l + \alpha_v = 1 \ ;$$

*Senior engineer in EDF, R&D, Fluid Dynamics, Power Generation and Environment, 6 quai Watier, 78400, Chatou, France.
†Research engineer, EDF, R&D, Fluid Dynamics, Power Generation and Environment, 6 quai Watier, 78400, Chatou, France.

The mean pressures, mean velocities and mean densities of the two phases are denoted P_ϕ, U_ϕ and ρ_ϕ respectively, for $\phi = l, v$. The total energy within each phase is:

$$E_\phi = \rho_\phi e_\phi(P_\phi, \rho_\phi) + \rho_\phi \frac{U_\phi^2}{2}, \qquad \phi = v, l \tag{1}$$

Internal energy functions e_ϕ must be provided by users.

The so-called conservative variable W will be defined as:

$$W = (\alpha_l, \alpha_l\rho_l, \alpha_l\rho_l U_l, \alpha_l E_l, \alpha_v\rho_v, \alpha_v\rho_v U_v, \alpha_v E_v)$$

Moreover, $P_I(W)$ and $V_I(W)$ respectively denote in this paper the interfacial pressure and velocity, and will be given afterwards. These interface terms V_I and P_I are such that:

- jump conditions are well defined within each isolated field;
- a physically relevant entropy inequality holds for smooth solutions of (2).

Given these notations, the governing set of equations for first-order moments may be written as follows in a one-dimensional framework:

$$\begin{cases} \partial_t(\alpha_l) + V_I\partial_x(\alpha_l) = S_{1,l} \\ \partial_t(\alpha_l\rho_l) + \partial_x(\alpha_l\rho_l U_l) = S_{2,l} \\ \partial_t(\alpha_l\rho_l U_l) + \partial_x\left(\alpha_l\rho_l U_l^2 + \alpha_l P_l\right) - P_I\partial_x(\alpha_l) = S_{3,l} \\ \partial_t(\alpha_l E_l) + \partial_x(\alpha_l U_l(E_l + P_l)) + P_I\partial_t(\alpha_l) = S_{4,l} \\ \partial_t(\alpha_v\rho_v) + \partial_x(\alpha_v\rho_v U_v) = -S_{2,l} \\ \partial_t(\alpha_v\rho_v U_v) + \partial_x\left(\alpha_v\rho_v U_v^2 + \alpha_v P_v\right) - P_I\partial_x(\alpha_v) = -S_{3,l} \\ \partial_t(\alpha_v E_v) + \partial_x(\alpha_v U_v(E_v + P_v)) + P_I\partial_t(\alpha_v) = S_{4,l} \end{cases} \tag{2}$$

where right-hand side terms $S_{k,l}(W)$ represent the source terms (for $k = 2, 3, 4$), which enable to account for mass transfer, momentum and energy transfer through the interface between the two phases. The term $S_{1,l}$ will also be introduced later on. Partial masses will be noted $m_\phi = \alpha_\phi\rho_\phi$.

A. Closure laws

Interfacial transfer contributions are defined as:

$$\begin{array}{l} S_{1,l} = (\tau_2)^{-1}\frac{\alpha_l\alpha_v}{P_l+P_v}(P_l - P_v) \\ S_{2,l} \overset{def}{=} \Gamma = (\tau_1)^{-1}\frac{1}{T_v^{-1}|g_v|+T_l^{-1}|g_l|}\frac{m_l m_v}{m_l+m_v}(T_v^{-1}g_v - T_l^{-1}g_l) \\ S_{3,l} = \mathcal{D} + (U_l + U_v)\Gamma/2 \\ S_{4,l} = (\tau_4)^{-1}\frac{m_l C_{V,l} m_v C_{V,v}}{m_l C_{V,l}+m_v C_{V,v}}(T_v - T_l) + (U_l + U_v)\mathcal{D}/2 + (U_l U_v)\Gamma/2 \end{array} \tag{3}$$

where free enthalpies g_ϕ and temperatures T_ϕ are defined as:

$$g_\phi = \left(e_\phi + \frac{P_\phi}{\rho_\phi}\right) - T_\phi s_\phi$$

$$1/T_\phi = \partial_{P_\phi}(s_\phi)/\partial_{P_\phi}(e_\phi)$$

Entropies s_ϕ should be chosen in agreement with the constraint:

$$(c_\phi)^2\partial_{P_\phi}(s_\phi) + \partial_{\rho_\phi}(s_\phi) = 0$$

The drag terms are modeled according to:

$$\mathcal{D} = (\tau_3)^{-1}\frac{m_l m_v}{m_l + m_v}(U_v - U_l)$$

These closure laws involve -positive- time scales which are noted τ_k (for $k = 1, .., 4$). We recall that:

$$C_{V,k} = \partial_{T_k} (e_k)_{|\rho_k} , \quad \text{for} \quad k = l, v.$$

Eventually, a keystone in the approach is hidden in a correct definition of the couple (V_I, P_I). We recall that the enforcement of a relevant entropy inequality has a straightforward consequence, which is that P_I may be written in terms of V_I and W *in a unique way.* The same holds when tackling three-phase flows, as emphasized in[17] . Now, a second requirement implies that the field associated with $\lambda = V_I$ should be linearly degenerate. As shown in[8,11] , few expressions guarantee this behaviour. Among these, one must point the following two:

- The so-called Baer-Nunziato closure, which corresponds to the choice $V_I = U_v$, and consequently $P_I = P_l$, owing to the previous remark ; this model is well suited for two-phase flows where the vapour is dilute ($\alpha_v << 1$) ;
- The mixture velocity closure, that is: $V_I = U_m \stackrel{def}{=} (m_l U_l + m_v U_v)/(m_l + m_v)$, and its corresponding value $P_I = \mu P_l + (1 - \mu)P_v$, setting $\mu = \frac{1}{1+m_l T_l/m_v T_v}$. Thus it corresponds in the asymptotic regime $T_v = T_l$ to $(m_v P_l + m_l P_v)/(m_v + m_l)$, which means that the interface pressure is mainly driven by the pressure of the vanishing phase P_v when m_v tends to 0. This closure is not relevant in our case.

Actually, an extended framework including the latter two formulations may be exhibited (see[18]).

From now on, we will restrict our attention to the first couple $(P_I, V_I) = (P_l, U_v)$.

B. Main properties

We may now recall in brief the main properties of system (2) using the previous closure laws. We emphasize that these are valid for above defined closure laws. The reader is refered to the references[8,11] (see also[17]) that contain all proofs, comments and details.

Property 1: (Hyperbolicity, structure of fields, entropy inequality and jump conditions)

- (1) The set of equations (2) is hyperbolic, since it admits seven real eigenvalues:

  $$\lambda_{1,2} = U_v, \quad \lambda_3 = U_v - c_v, \quad \lambda_4 = U_v + c_v, \quad \lambda_5 = U_l, \quad \lambda_6 = U_l - c_l, \quad \lambda_7 = U_l + c_l$$

  and associated righteigenvectors span the whole space $\mathcal{R}^7$, unless $|U_l - U_v|/c_l = 1$;
- (2) Fields associated with eigenvalues $\lambda_{1,2,5}$ are linearly degenerate. Other fields are genuinely non linear;
- (3) Within each isolated field associated with λ_k, unique jump conditions hold. Apart from the field associated with the eigenvalue $\lambda = U_v$, α_l is uniform and thus these jump conditions correspond to single phase jump relations, that is:

  $$\begin{array}{l} -\sigma[\rho_\phi]_l^r + [\rho_\phi U_\phi]_l^r = 0; \\ -\sigma[\rho_\phi U_\phi]_l^r + [\rho_\phi U_\phi^2 + P_\phi]_l^r = 0; \\ -\sigma[E_\phi]_l^r + [U_\phi(E_\phi + P_\phi)]_l^r = 0, \end{array} \tag{4}$$

  where σ denotes the speed of the sock wave, and l, r the left-right states on each side of this travelling discontinuity.
- (4) Define the entropy $\eta(W) = m_l s_l + m_v s_v$ and the entropy flux $f_\eta(W) = m_l s_l U_l + m_v s_v U_v$; then smooth solutions W of (2) are such that:

  $$0 \leq \partial_t (\eta(W)) + \partial_x (f_\eta(W)) . \tag{5}$$

Obviously, the structure of the $1, 2$-field is crucial in order to obtain unique jump conditions. This is not clear in the literature according to the authors. We now provide the whole algorithm that is used in order to obtain approximate solutions of system (2).

III. Numerical algorithm

We use a fractional step method that complies with the entropy inequality (5) ; a first "evolution" step accounts for all convective effects, while the second "relaxation" step takes source terms into account.

- *Evolution step*
  This step computes approximate solutions of the hyperbolic homogeneous system:

$$\left\{\begin{array}{l} \partial_t\left(\alpha_l\right)+V_I\partial_x\left(\alpha_l\right)=0 \\ \partial_t\left(\alpha_l\rho_l\right)+\partial_x\left(\alpha_l\rho_l U_l\right)=0 \\ \partial_t\left(\alpha_l\rho_l U_l\right)+\partial_x\left(\alpha_l\rho_l U_l^2+\alpha_l P_l\right)-P_I\partial_x\left(\alpha_l\right)=0 \\ \partial_t\left(\alpha_l E_l\right)+\partial_x\left(\alpha_l U_l(E_l+P_l)\right)+P_I\partial_t\left(\alpha_l\right)=0 \\ \partial_t\left(\alpha_v\rho_v\right)+\partial_x\left(\alpha_v\rho_v U_v\right)=0 \\ \partial_t\left(\alpha_v\rho_v U_v\right)+\partial_x\left(\alpha_v\rho_v U_v^2+\alpha_v P_v\right)-P_I\partial_x\left(\alpha_v\right)=0 \\ \partial_t\left(\alpha_v E_v\right)+\partial_x\left(\alpha_v U_v(E_v+P_v)\right)+P_I\partial_t\left(\alpha_v\right)=0 \end{array}\right. \tag{6}$$

  through the time interval $[t^n, t^n+\Delta t]$, with given initial values W^n, using a Finite Volume scheme to be defined. This provides a set of approximations $\tilde{W}$.

- *Relaxation step*
  Given discrete cell values of $\tilde{W}$, we compute approximations of the coupled set of ODEs corresponding to relaxation terms, that is:

$$\left\{\begin{array}{l} \partial_t\left(\alpha_l\right)=S_{1,l} \\ \partial_t\left(\alpha_l\rho_l\right)=S_{2,l} \\ \partial_t\left(\alpha_l\rho_l U_l\right)=S_{3,l} \\ \partial_t\left(\alpha_l E_l\right)+P_I\partial_t\left(\alpha_l\right)=S_{4,l} \\ \partial_t\left(\alpha_v\rho_v+\alpha_l\rho_l\right)=0 \\ \partial_t\left(\alpha_v\rho_v U_v+\alpha_l\rho_l U_l\right)=0 \\ \partial_t\left(\alpha_v E_v+\alpha_l E_l\right)=0 \end{array}\right. \tag{7}$$

Approximate solutions in the evolution step are obtained using either the non-conservative form of Rusanov scheme, or the non-conservative form of the approximate Godunov scheme VFRoe-ncv[6] . We refer to[10,11,21] for such a description. Of course, other solvers have been proposed for such a purpose, among which we may cite those that are detailed in the papers[1,2,7] , which are grounded on the use of relaxation techniques, but also approximate Riemann solvers such as those detailed in[24,26,30,31] . One must be aware here that the approximation of shock solutions makes sense for system (6), though the system has no conservative form, since first-order non-conservative products are only active in linearly degenerate fields. A straightforward consequence is that we expect schemes to converge towards the same solution when the mesh is refined (see[16] for instance which examines this specific point).

We detail afterwards the relaxation step, with special focus on the computation of mass transfer terms. This relaxation step is in fact split into four substeps through which one accounts for drag effects, heat exchange, pressure relaxation effects and mass transfer respectively.

1. Velocity relaxation step

This step accounts for drag terms only. Starting with an initial condition indexed by n, the following update is achieved, which provides new values indexed by $n, *$:

$$\begin{cases} \alpha_l^{n,*} = \alpha_l^n, \\ m_l^{n,*} = m_l^n, \\ m_v^{n,*} = m_v^n, \\ U_l^{n,*} = U_l^n + (U_v^n - U_l^n)\frac{m_v^n(1-e^{(-\Delta t/\tau_3^n)})}{m_l^n+m_v^n}, \\ U_v^{n,*} = U_v^n - (U_v^n - U_l^n)\frac{m_l^n(1-e^{(-\Delta t/\tau_3^n)})}{m_l^n+m_v^n}, \\ (m_l e_l)^{n,*} = (m_l e_l)^n + \frac{m_l^n m_v^n}{m_l^n+m_v^n}\frac{(U_l^n-U_v^n)^2}{2}(1-e^{(-2\Delta t/\tau_3^n)}), \\ (m_v e_v)^{n,*} = (m_v e_v)^n. \end{cases} \tag{8}$$

Of course, the void fraction and partial masses remain unchanged through this velocity relaxation step, and the total mean momentum and the mean total energy are also preserved. It may be easily checked that internal energies remain positive through this substep.

2. Temperature relaxation step

Once again, both the void fraction and the partial masses remain steady through this step which computes approximations of solutions of system:

$$\begin{cases} \partial_t(\alpha_l) = 0 \\ \partial_t(\alpha_l\rho_l) = 0 \\ \partial_t(\alpha_l\rho_l U_l) = 0 \\ \partial_t(\alpha_l E_l) = (\tau_4)^{-1}\frac{m_l C_{V,l} m_v C_{V,v}}{m_l C_{V,l}+m_v C_{V,v}}(T_v - T_l) \\ \partial_t(\alpha_v\rho_v + \alpha_l\rho_l) = 0 \\ \partial_t(\alpha_v\rho_v U_v + \alpha_l\rho_l U_l) = 0 \\ \partial_t(\alpha_v E_v + \alpha_l E_l) = 0 \end{cases} \tag{9}$$

The temperature relaxation scheme updates internal energies at time $n, **$ according to the rule:

$$\begin{cases} \alpha_l^{n,**} = \alpha_l^{n,*} \\ m_k^{n,**} = m_k^{n,*} \qquad \text{for } k = l, v \\ m_k^{n,**}U_k^{n,**} = m_k^{n,*}U_k^{n,*} \qquad \text{for } k = l, v \\ m_l^{n,*}(e_l^{n,**} - e_l^{n,*}) = \frac{\Delta t}{\theta^{n,*}}(T_v(e_v^{n,**}, \rho_v^{n,*}) - T_l(e_l^{n,**}, \rho_l^{n,*})) \\ m_v^{n,*}(e_v^{n,**} - e_v^{n,*}) + m_l^{n,*}(e_l^{n,**} - e_l^{n,*}) = 0 \end{cases} \tag{10}$$

where $\theta^{n,*} = (\tau_4)^{n,*}(\frac{m_l C_{V,l}+m_v C_{V,v}}{m_l C_{V,l} m_v C_{V,v}})^{n,*}$. Thus this step requires solving a non-linear system of two unknowns $(e_v^{n,**}, e_l^{n,**})$. However, it performs better than some other linearized schemes.

3. Pressure relaxation step

The pressure relaxation step computes approximations of solutions of the ODEs:

$$\begin{cases} \partial_t(\alpha_l) = S_{1,l} \\ \partial_t(m_\phi) = 0 \\ \partial_t(m_\phi U_\phi) = 0 \\ \partial_t(m_l e_l) + P_l\partial_t(\alpha_l) = 0 \\ \partial_t(\alpha_v E_v + \alpha_l E_l) = 0 \end{cases} \tag{11}$$

with $\phi = l, v$. Two distinct schemes have been proposed in[20] in order to cope with (11). Both guarantee positive values of void fractions α_ϕ and a perfect balance of total energies. The first one is a semi-implicit

scheme, that is such that the existence and uniqueness of the discrete solution is ensured, whatever the equations of state would be. The second one is totally implicit with respect to the unknown (P_l, P_v, α_l).

We only detail herein the second one which calculates $(P_l, P_v, \alpha_l)^{n,***}$ solution of the implicit step:

$$\left\{\begin{array}{l} \alpha_l^{n,***} - \alpha_l^{n,**} = \frac{\Delta t}{\tau_2^{n,**}} \alpha_l^{n,***} \alpha_v^{n,***} (P_l^{n,***} - P_v^{n,***})/(P_l^{n,**} + P_v^{n,**}) \\ m_k^{n,***} = m_k^{n,**} \qquad \text{for } k = l, v \\ m_k^{n,***} U_k^{n,***} = m_k^{n,**} U_k^{n,**} \qquad \text{for } k = l, v \\ m_l^{n,**}(e_l^{n,***} - e_l^{n,**}) + P_l^{n,***}(\alpha_l^{n,***} - \alpha_l^{n,**}) = 0 \\ m_v^{n,**}(e_v^{n,***} - e_v^{n,**}) + m_l^{n,**}(e_l^{n,***} - e_l^{n,**}) = 0 \end{array}\right. \tag{12}$$

using abusive notations: $e_\phi^{n,***} = e_\phi(P_\phi^{n,***}, \rho_\phi^{n,***})$, and $\rho_\phi^{n,***} = m_\phi^{n,***}/\alpha_\phi^{n,***}$. Conditions that guarantee the existence and uniqueness of the solution $(P_l, P_v, \alpha_l)^{n,***}$ are detailed in[20] . Actually, this algorithm is exactly the same as the one introduced in[10] . We refer the reader to the latter reference, which examines the mesh refinement effects when $\tau_2 = \epsilon << 1$ and when $\tau_2 = 0$ respectively, using meshes with up to 10^6 cells. As expected, this enables to retrieve the fact that the initial-value problem associated with system (2) and $\tau_2 = 0$ is ill-posed (see[19] and[16] also for a similar study). We also recall that a simpler algorithm was proposed in[11] in order to compute approximations of the pressure relaxation substep (11) ; however, a drawback of this algorithm is that it does not ensure the exact conservation of the total energy of the mixture.

4. Taking mass transfer into account

The last relaxation step takes mass tranfer terms into account. It is indeed an important step, and the algorithm which is used is the following. Starting with values $W_\phi^{n,***}$ issuing from the pressure relaxation step, and noting formally this time as $t = 0$, the Gibbs potential desequilibrium and the relaxation time are frozen at the beginning of the time step, defining Γ as follows :

$$\Gamma = \frac{G(0)}{\tau_1(0)} \frac{m_l m_v}{m_l + m_v}.$$

with an obvious definition of G in agreement with formula (3):

$$G = \frac{(T_v^{-1} g_v - T_l^{-1} g_l)}{T_v^{-1}|g_v| + T_l^{-1}|g_l|}$$

Hence, we rewrite the step as:

$$\left\{\begin{array}{l} \partial_t(\alpha_l) = 0 \\ \partial_t(m_l) = \Gamma \\ \partial_t(m_l U_l) = \Gamma(U_l + U_v)/2 \\ \partial_t(\alpha_l E_l) = \Gamma(U_l U_v)/2 \\ \partial_t(m_v + m_l) = 0 \\ \partial_t(m_v U_v + m_l U_l) = 0 \\ \partial_t(\alpha_v E_v + \alpha_l E_l) = 0 \end{array}\right. \tag{13}$$

and a direct time integration yields:

$$m_l(t) = m_l(0) \frac{(m_l(0) + m_v(0)) e^{(tG(0)/\tau_1(0))}}{m_l(0) e^{(tG(0)/\tau_1(0))} + m_v(0)} \quad \text{and} \quad m_v(t) = m_v(0) \frac{m_l(0) + m_v(0)}{m_l(0) e^{(tG(0)/\tau_1(0))} + m_v(0)}.$$

It must be emphasized that a straightforward consequence of this choice of algorithm is that partial masses remain positive through the step, without any constraint on the time step. The update of momentum $m_l U_l, m_v U_v$ and total energies E_v, E_l is straightforward, and of course the conservation of the mass, momentum and total energy of the mixture is preserved. It must be emphasized that the potential desequilibrium is taken into account in an explicit way in the latter scheme, so that one may conjecture that a more robust scheme grounded on an implicit formulation might be built later on.

IV. Numerical results

We recall first very briefly in the following two subsections some previous results that have been obtained while computing the evolution step and the pressure-velocity-temperature relaxation step. Then we present a few numerical results in some particular situations.

A. Validation of the evolution step

We do not detail this part here and we refer to[9, 13, 25, 28] where many simulations of one-dimensional Riemann problems are reported, by computing the L^1 norm of the error, considering meshes with up to 5.10^5 regular cells. We emphasize that the expected asymptotic rate of convergence is $h^{1/2}$ (resp. $h^{2/3}$) for first-order (resp. second-order) schemes, due to the occurence of the contact waves associated with U_v and U_l; actually, this is precisely what is retrieved in the above-mentionned references when the mesh size is refined, at a given CFL number (typically $CFL = 1/2$).

B. Validation of the pressure-velocity-temperature relaxation step

We refer to[20, 21] which focus on the validation of the pressure-velocity-temperature relaxation step. Specific analytical solutions have been used in these reports in order to estimate true rates of convergence. The latter references also provide theoretical conditions in order to ensure existence and uniqueness of solutions of coupled discrete problems associated with the pressure and temperature relaxation steps. Quite surprinsingly, the computation of this step is not very well documented in the known literature, though the relaxation step is stiff and involves highly non-linear effects between all components of the state variable W.

C. Two-dimensional simulation of a heated wall

We consider the two-dimensional unsteady computation of a heated wall in an almost square domain, where the wall contains a small cavity -in the lower part- (see figure 1). The computational domain contains

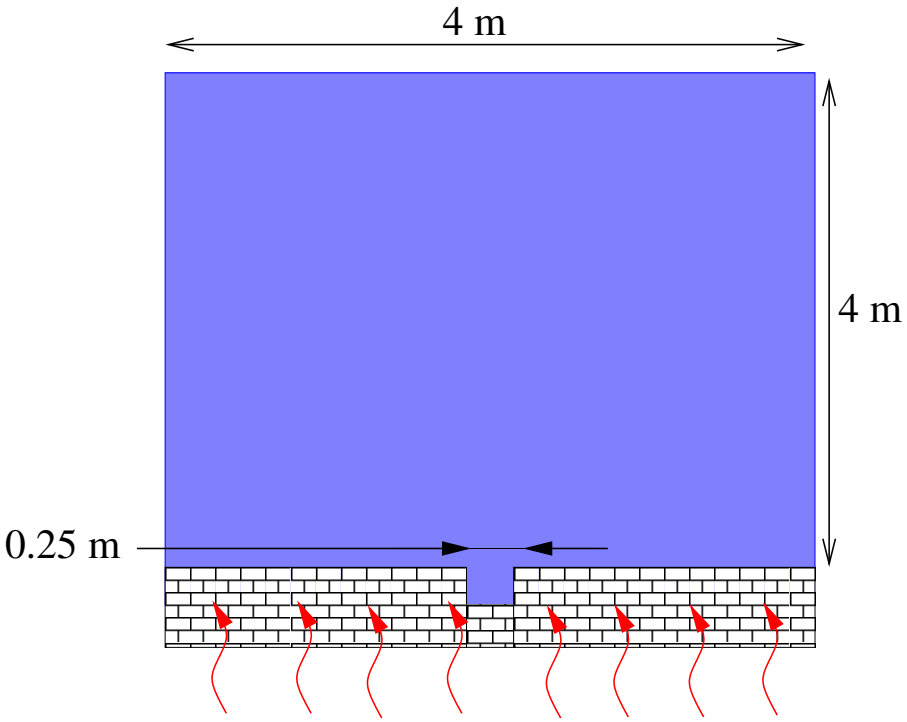

Figure 1. Heated wall: sketch of the computational domain

10^5 regular cells, and the CFL number is set to 1/2. Homogeneous Neumann-type boundary conditions

have been used on the left, right and upper boundaries. The relaxation time scales are constant in this experiment: $\tau_1 = 10^{-6}$, $\tau_2 = 10^{-5}$, $\tau_3 = 10^{-4}$, $\tau_4 = 10^{-6}$. Uniform initial conditions are such that the fluid is at rest at the beginning of the computation, which means that: $\rho_l(x,y,0) = 765.$, $\rho_v(x,y,0) = 76.$, $P_l(x,y,0) = P_v(x,y,0) = 166 \times 10^5$, $U_l^x(x,y,0) = U_v^x(x,y,0) = 0$ and $U_l^y(x,y,0) = U_v^y(x,y,0) = 0$. The liquid mass fraction has been set to 0.95, and we use perfect gas EOS within each phase, setting: $\gamma_v = 1.4$ and $\gamma_l = 1.038$. The normal heat flux is uniform along the wall direction, and its steady value is: $HF = 10^6 J/s/m^2$. The final time of the computation is $T = 2.375 \times 10^{-2}$, and the average time step at the end of the computation is approximately equal to $\Delta t = 4.8 \times 10^{-6}$. Figures 2 and 3 show the liquid void fraction and liquid pressure isolines at the end of the computation.

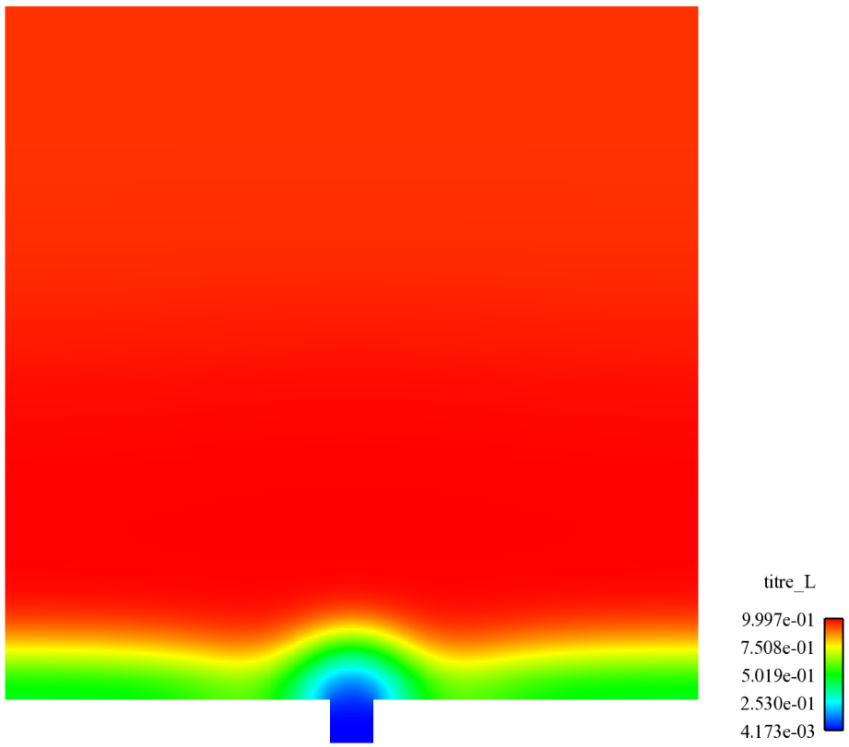

Figure 2. Heated wall: contours of the liquid void fraction α_l at time $T = 0.0237$.

D. Interfacial mass transfer in a stratifying layer

Eventually, we discuss a one-dimensional test case corresponding to a vertical stratification of an initially homogeneous medium, following[11] , while including mass transfer effects. Thus we consider a homogeneous mixture initially at rest ($U_v(t=0) = U_l(t=0) = 0$) with ambient conditions ($P_l(t=0) = P_v(t=0) = 101300Pa$, and $\rho_l(t=0) = 1000$, $\rho_v(t=0) = 1$), while setting a uniform value $\alpha_l(t=0) = 0.5$. The relaxation time scale in the mass transfer term is now $\tau_1 = 10^{-4}$, and we set $\tau_2 = 5 \times 10^{-4}$, $\gamma_v = 1.4$, $\gamma_l = 1.0005$. Following[11] , both drag effects and heat transfer are neglected, thus $(\tau_3)^{-1} = (\tau_4)^{-1} = 0$. The gravity constant is set to $g = 9.81$, and the computational domain is $[0,5]$. A stratification develops, which is represented in figures 4 and 5, which display the statistical fraction of the liquid phase, and the relative Mach number $|U_v - U_l|/c_l$ respectively. In figure 4, a mesh refinement (with $200, 500, 2000$ regular cells) shows strong variations of the front shapes at time $t = 0.05$; moreover, gradients increase when the mass transfer is taken into account ($\tau_1 = 10^{-4}$) or not ($\tau_1 = +\infty$). Figure 5 clearly gives some numerical evidence that some resonance phenomenon has occured at the beginning of the computation. Computations on finer meshes confirm this point. This phenomenon disappears when drag effects are taken into account.

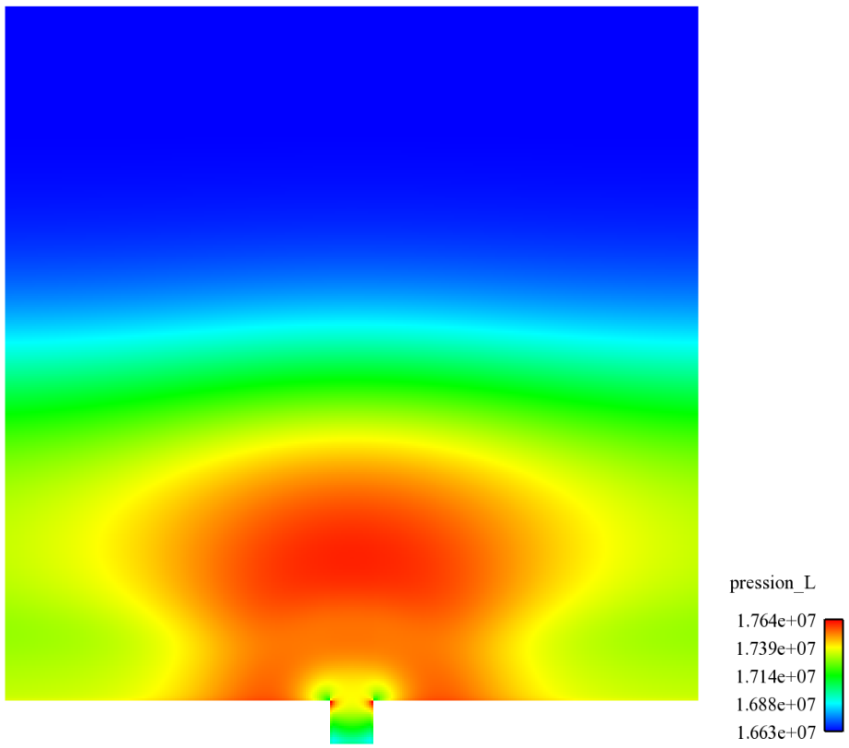

Figure 3. Heated wall: contours of the liquid pressure P_l at time $T = 0.0237$.

E. Simulation of the flow in a heated pipe

We consider now the one-dimensional flow in a long pipe which is uniformly heated on its lateral boundaries. The heat flux is $HF = 2.5 \times 10^6 J/m^2/s$; the EOS in the vapour phase is: $P_v = (\gamma_v - 1)\rho_v e_v$, while the liquid EOS is: $P_l + \gamma_l \pi_l^\infty = (\gamma_l - 1)\rho_l e_l$, where $\gamma_v = 1.249$, $\gamma_l = 1.853$ and $\pi_l^\infty = 1.038 \times 10^9$; besides, we use $(C_v)_l = 3142$ and $(C_v)_v = 1925$. Pressure and velocity relaxation time scales are set to $\tau_2 = \tau_3 = 10^{-9}$. The mesh contains 420 regular cells, the CFL constraint is $CFL = 1/2$, and the heat flux is enforced only if x is in the range $[50, 370]$. Initial conditions are uniform in the pipe and such that : $\alpha_l(x, 0) = 0.995$, $P_l(x, 0) = P_v(x, 0) = 40 \times 10^5$, $U_l(x, 0) = U_v(x, 0) = 5$, $\rho_l(x, 0) = 919$ and $\rho_v(x, 0) = 20$. The inlet boundary condition is exactly equal to the initial condition.

Figure 6 shows profiles at time $T = 5$ for α_l, $m_l/(m_l + m_v)$, ρ_l, ρ_v, P_l and U_l, when no masss tranfer is allowed between phases ($\tau_1 = 10^9$). Two small shock waves may be observed in the pressure profiles around the inlet and the outlet of the heated zone. The liquid pressure (bottom left) decreases in this region, while the liquid velocity (bottom right) increases in a linear way. We observe rather weak discrepancies whenever the interphase heat exchange is weak (plain line in figure 6) or higher (dashed line in figure 6); in both cases, the density of the liquid phase diminishes in the heated region. As expected, liquid and vapour velocities -and pressures- hardly differ.

Figure 7 provides similar results when the mass transfer occurs ($\tau_1 = 10^{-3}$). The main difference that arises concerns the vapour profile of the density. The sensitivity to the heat exchange is also emphasized due to the competition with the mass transfer.

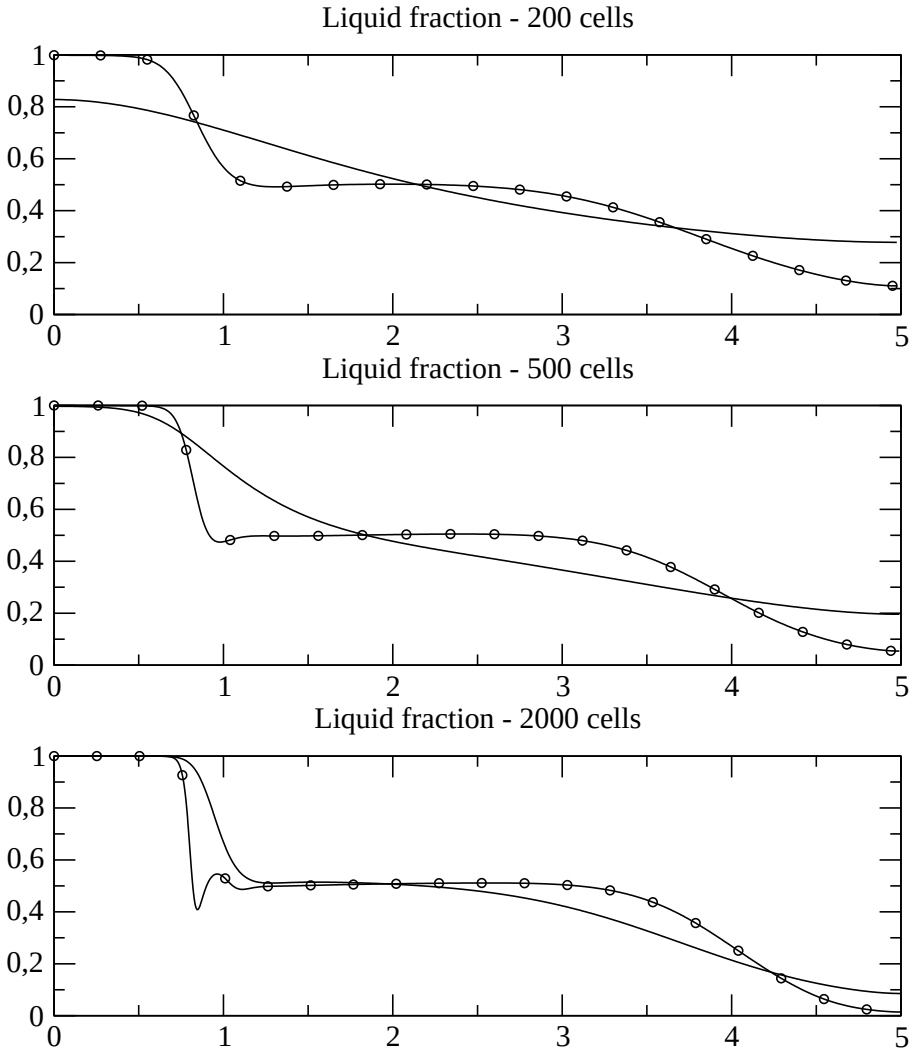

Figure 4. Stratified layer: liquid void fraction profiles for α_l at time $T = 0.05$. Straight line: without mass transfer, circles: with mass transfer.

Conclusion

We have presented in this paper a fractional step method that is used in order to compute approximations of a two-fluid model with mass transfer. We emphasize that:

- (i) the computation of stable and accurate approximations of the homogeneous convective part is still a difficult problem, though many efforts in that direction arise in the two-phase flow community,
- (ii) the approximation of solutions of the coupled set of ODEs which govern pressure relaxation effects is indeed tricky due to the strong coupling of the governing equations of the statistical void fraction and the total energies,
- (iii) taking mass transfer into account is also a key point, of crucial importance for water-vapour applications such as those occuring in pressurised water reactors, and the distinct small relaxation time scales render the problem even more tricky.

These three items require further developments and investigation in order to get reliable enough algorithms.

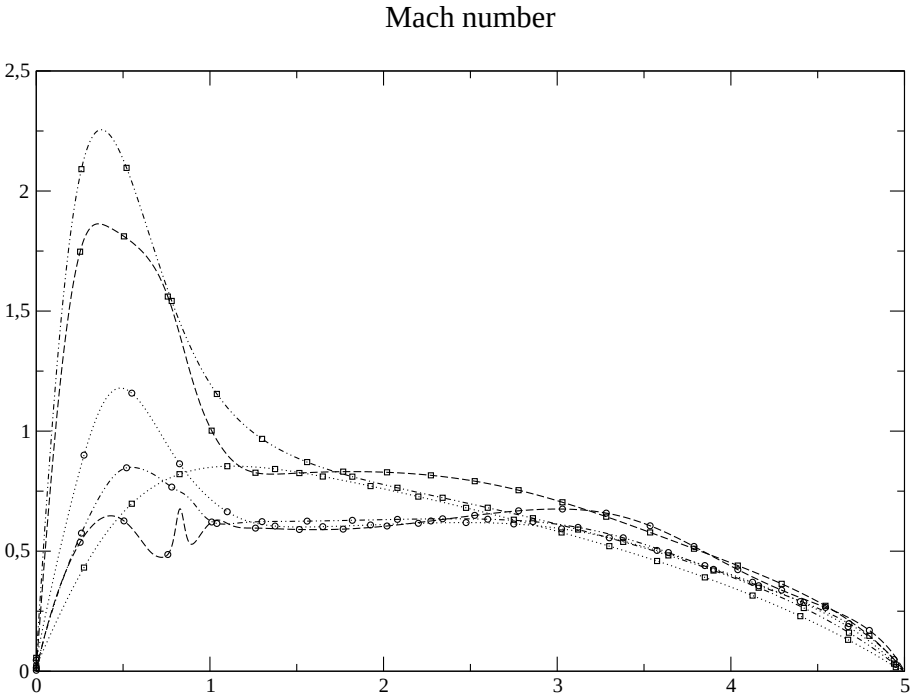

Figure 5. Stratified layer: relative Mach number $(U_v - U_l)/c_l$ at different times $T = 0.004$ (dotted line), $T = 0.01$ (dotted-dashed line), $T = 0.05$ (dashed line). Circles: with mass transfer, squares: without mass transfer.

Acknowledgments:

This work has been achieved in the framework of the NEPTUNE project[15] , with financial support by CEA (Commissariat à l'Energie Atomique et aux Energies Alternatives), EDF, IRSN (Institut de Radioprotection et de Sureté Nucléaire) and AREVA-NP.

References

[1] Ambroso, A., Chalons, C., Coquel, F., and Galié, T., "Relaxation and numerical approximation of a two-fluid two-pressure diphasic model " *Math. Model. and Numer. Anal.*, vol. 43(6), 2009, pp. 1063–1098.

[2] Ambroso, A., Chalons, C., and Raviart, P.A., "A Godunov-type method for the seven-equation model of compressible two-phase flow " *Computers and Fluids*, vol. 54, 2012, pp. 67-91.

[3] Andrianov, N., and Warnecke, G., " The Riemann problem for the Baer-Nunziato two-phase flow model", *J. Comp. Physics.*, vol. 195, 2004, pp. 434-464.

[4] Baer, M.R., and Nunziato, J.W., "A two-phase mixture theory for the deflagration to detonation transition (DDT) in reactive granular materials", *Int. J. Multiphase Flow*, vol. 12(6), 1986, pp. 861–889.

[5] Bdzil, J.B., Menikoff, R., Son, S.F., Kapila, A.K., and Stewart, D.S., "Two-phase modeling of a DDT in granular materials: a critical examination of modeling issues", *Phys. of Fluids*, vol. 11, 1999, pp. 378-402.

[6] Buffard, T., Gallouët, T., and Hérard, J.-M., "A sequel to a rough Godunov scheme. Application to real gases ", *Computers and Fluids*, vol. 29(7) , 2000, pp. 813-847.

[7] Chalons, C., Coquel, F., Kokh, S., and Spillane, N. "A relaxation method to compute approximations of the Baer-Nunziato model" *Proceedings of Finite Volumes Complex Applications VI*, Fort, Furst, Halama, Herbin, Hubert editors, Springer-Verlag, 2011.

[8] Coquel, F., Gallouët, T., Hérard, J.M., and Seguin, N., "Closure laws for a two-fluid two-pressure model", *C. R. Acad. Sci. Paris*, vol. I-332, 2002, pp. 927–932.

[9] Crouzet F., Daude F., Galon P., Helluy P., Hérard J.M., Liu Y., "On the computation of the Baer-Nunziato model", *contribution to the 42nd AIAA FD conference*, 2011.

[10] Gallouët, T., Helluy, P., Hérard, J.-M., and Nussbaum, J., "Hyperbolic relaxation models for granular flows", *Math. Model. and Numer. Anal.*, vol.44(2), 2010, pp.371-400.

[11] Gallouët, T., Hérard, J.-M., and Seguin, N., "Numerical modelling of two phase flows using the two-fluid two-pressure approach", *Math. Mod. Meth. in Appl. Sci.*, vol. 14(5), 2004, pp. 663-700.

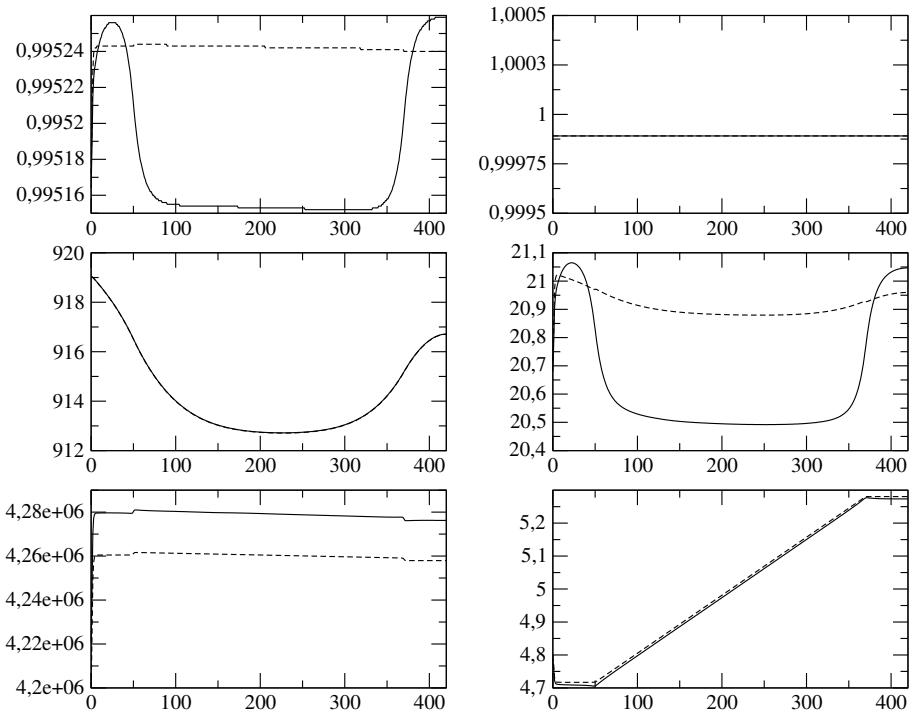

Figure 6. Heated pipe without any mass transfer: profiles along the main axis of: α_l (top left), $m_l/(m_l+m_v)$ (top right), ρ_l (medium left), ρ_v (medium right), P_l (bottom left), U_l (bottom right), at time $T=5$. Plain line: weak interphase heat transfer ($\tau_4=10^{-1}$), dashed line: high interphase heat transfer ($\tau_4=10^{-5}$).

[12] Gavrilyuk, S., and Saurel, R., "Mathematical and numerical modelling of two phase compressible flows with inertia", *J. Comp. Physics.*, vol. 175, 2002, pp. 326-360.

[13] Girault, L., and Hérard, J.-M., "A two-fluid hyperbolic model in a porous medium", *Math. Model. and Numer. Anal.*, vol. 44(6), 2010, pp. 1319-1348.

[14] Godunov, S.K., "Finite difference method for numerical computation of discontinuous solutions of the equations of fluid dynamics", *Mat. Sb.*, vol. 47, 1959, pp. 271-300.

[15] Guelfi, A., Bestion, D., Boucker, M., Boudier, P., Fillion, P., Grandotto, M., Hérard, J.M., Hervieu, E., and Peturaud, P., "Neptune: a new software platform for advanced nuclear thermal hydraulics", *Nuclear Science Engineering*, vol. 156, 2007, pp. 281-324.

[16] Guillemaud, V., "Modélisation et simulation numérique d'écoulements diphasiques par une approche bifluide à deux pressions", *PhD thesis*, Université Aix-Marseille I, Marseille, France, 2007.

[17] Hérard, J.-M., "A three-phase flow model", *Mathematical Computer Modelling*, vol. 45, 2007, pp. 432-455.

[18] Hérard, J.-M., "Une classe de modèles diphasiques bi-fluides avec changement de régime", *internal EDF report*, H-I81-2010-0486-FR, in French, 2010.

[19] Hérard, J.-M., and Hurisse, O., "A simple method to compute standard two-fluid models", *Int. J. Comput. Fluid Dynamics*, vol. 19(7), 2005, pp. 475-482.

[20] Hérard, J.-M., and Hurisse, O., "Schémas d'intégration du terme source de relaxation des pressions phasiques pour un modèle bifluide hyperbolique", *EDF report*, H-I81-2009-1514-FR, in French, 2009.

[21] Hérard, J.-M., and Hurisse, O., " A fractional step method to compute a class of compressible gas-liquid flows", *Computers and Fluids*, vol. 55, 2012, pp. 57-69.

[22] Kapila, A.K., Menikoff, R., Bdzil, J.B., Son, S.F., and Stewart, D.S., "Two-phase modeling of a DDT in granular materials: reduced equations", *Phys. of Fluids*, vol. 13, 2001, pp. 3002-3024.

[23] Kapila, A.K., Son, S.F., Bdzil, J.B., Menikoff, R., and Stewart, D.S., "Two-phase modeling of a DDT: structure of the velocity relaxation zone", *Phys. of Fluids*, vol. 9(12), 1997, pp. 3885–3897.

[24] Karni, S., and Hernandez-Duenas, G., "A hybrid algorithm for the Baer Nunziato model using the Riemann invariants", *SIAM J. of Sci. Comput.*, vol.45, 2010, pp.382-403.

[25] Liu, Y., PhD thesis, Université Aix Marseille I, Marseille, France, *in preparation*, 2013.

[26] Lowe, C.A., " Two-phase shock-tube problems and numerical methods of solution", *J. Comp. Physics.*, vol. 204, 2005, pp. 598-632.

[27] Ransom, V., and Hicks, D.L., "Hyperbolic two-pressure models for two-phase flow", *J. Comp. Physics.*, vol. 53, 1984, pp. 124-151.

[28] Saleh, K., PhD thesis, Université Pierre et Marie Curie, Paris, France, *in preparation*, 2012.

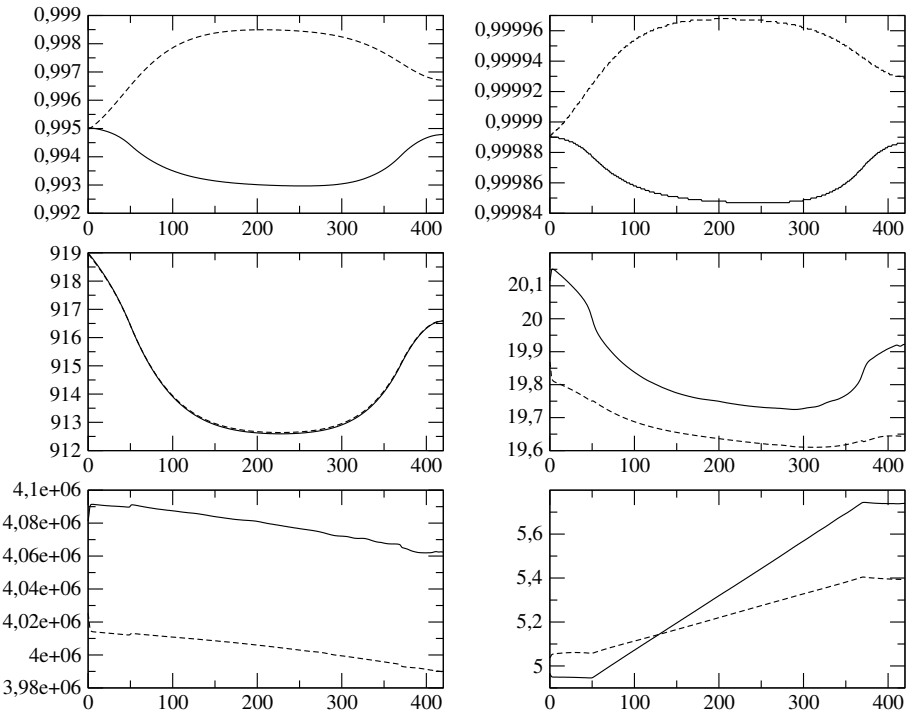

Figure 7. Heated pipe with mass transfer: profiles along the main axis of: α_l (top left), $m_l/(m_l + m_v)$ (top right), ρ_l (medium left), ρ_v (medium right), P_l (bottom left), U_l (bottom right), at time $T = 5$. Plain line: weak interphase heat transfer ($\tau_4 = 10^{-1}$), dashed line: high interphase heat transfer ($\tau_4 = 10^{-5}$).

[29] Saurel, R., and Abgrall, R., " A Multiphase Godunov Method for Compressible Multifluid and Multiphase Flows ", *J. Comp. Physics.*, vol. 150, 1999, pp. 425-467.

[30] Schwendeman, D.W., Wahle, C.W., and Kapila, A.K., " The Riemann problem and a high-resolution Godunov method for a model of compressible two-phase flow ", *J. Comp. Physics.*, vol. 212, 2006, pp. 490-526.

[31] Tokareva, S.A., and Toro, E.F., " HLLC type Riemann solver for the Baer-Nunziato equations of compressible two-phase flow", *J. Comp. Physics.*, vol. 229, 2010, pp. 3573-3604.